Interference and Throughput in Spectrum Sensing Cognitive Radio Networks using Point Processes

Anthony Busson, Bijan Jabbari, Alireza Babaei, and Véronique Vèque

Abstract: **Spectrum sensing is vital for secondary unlicensed nodes to coexist and avoid interference with the primary licensed users in cognitive wireless networks. In this paper, we develop models for bounding interference levels from secondary network to the primary nodes within a spectrum sensing framework. Instead of classical stochastic approaches where Poisson point processes are used to model transmitters, we consider a more practical model which takes into account the medium access control regulations and where the secondary Poisson process is judiciously thinned in two phases to avoid interference with the secondary as well as the primary nodes. The resulting process will be a modified version of the Matérn point process. For this model, we obtain bounds for the complementary cumulative distribution function of interference and present simulation results which show the developed analytical bounds are quite tight. Moreover, we use these bounds to find the operation regions of the secondary network such that the interference constraint is satisfied on receiving primary nodes. We then obtain theoretical results on the primary and secondary throughputs and find the throughput limits under the interference constraint.**

Index Terms: **Cognitive radio, performance evaluation, stochastic geometry.**

I. INTRODUCTION

Dynamic spectrum access and management provides an opportunity to use the limited radio frequency more efficiently. This is irrefutably needed as there is a growing demand for higher transmission rates and increased network throughput. While this notion, in general, encompasses a variety of wireless systems, one important scenario of interest is the concept in which the unlicensed users are allowed to access the spectrum licensed to the incumbent users on a non-interfering or limited interference basis. The practical solution requires wireless devices with cognitive radio capability to share the bandwidth with primary users.

Considerable research has been undertaken in the area of dynamic spectrum access and management and cognitive networks (see for example, [1]–[5]). To implement such systems, various approaches have been discussed that involve issues ranging from spectrum opportunity identification and exploitation to medium access control (MAC) protocol [6]. One important component of the cognitive radio technology is the spectrum sensing [7]. Spectrum sensing enables the secondary nodes to be perceptive of the spectral activity of the primary users and thereby avoid and manage their level of interference. Different approaches have been proposed for spectrum sensing ranging from energy detection [8] and cyclostationarity-based sensing to cooperative spectrum sensing [7], [9].

What gives rise to such concepts to become realistic is managing the level of interference being harmful to the incumbent users. Therefore, an understanding of the characteristics of interference and its behavior is at the core of the problem of determining the degree of bandwidth efficiency and hence useful capacity to be used by secondary nodes. Given that the primary and secondary wireless networks share the space and the spectrum, throughput in both of these networks is limited by not only the intra-network interference, i.e., the interference among the nodes of the same network, but also by the inter-network interference, i.e., the aggregate interference originated from transmitting nodes in one network on the receiving nodes of the other network [10]. On the other hand, due to the factors like randomness in the locations of the primary and the secondary nodes, the type of MAC layer protocols and the scheduling algorithms used in these networks which determine the simultaneous transmitters, as well as the fading effect, the intra-network and inter-network interference, and their cumulated effect are random in nature. Therefore, statistical characterization of interference is an important prerequisite for modeling and optimization of throughput in the primary and secondary networks. This is precisely our focus here and we develop analytical models and bounds for the level of interference in order to evaluate the impact of secondary transmissions on the primary network and determine the throughput.

In [11], the authors show that there is a fundamental trade-off between sensing capability (a function of probability of detection in spectrum sensing) and achievable throughput (a function of probability of false alarm in spectrum sensing) and obtains the optimal sensing duration which maximizes the throughput in the secondary network under the constraint that the primary users are sufficiently protected. Only a single point-to-point transmission link in the secondary network is considered and the effect of interference among secondary nodes is ignored. [12] considers the problem of maximizing the sum-throughput in the secondary network subject to constraints on maximum interference at primary receivers. The network is assumed to be comprised of a finite number of nodes and that nodes have perfect knowledge of primary-secondary and secondary-secondary path gains. This model does not consider the inherent uncertainty in path gains due to random propagation effects and the randomness in the spatial distribution of nodes. [13] considers interference model-

Manuscript received September 28, 2012; approved for publication by Sengoku, Masakazu, Division II Editor, December 9, 2013

Anthony Busson is with the University at Lyon 1, 46 Allée d'Italie Lyon 69364 France. email: anthony.busson@inria.fr.

Bijan Jabbari is with the Department of Electrical and Computer Engineering at George Mason University, Fairfax, Virginia, USA.

Alireza Babei is with the Auburn University.

Véronique Vèque is with the University Paris XI.

Digital object identifier 10.1109/JCN.2014.000010

ing in spectrum underlay cognitive wireless networks and interference is approximated as sum of normal and log-normal random variables. In [10], considering a simple Gaussian model, throughput in primary and secondary networks is optimized by using the optimum transmission probability. In [14], the authors present a cognitive radio system for which they propose a power allocation strategy that optimizes throughput under interference power constraints on the primary network. In [15] and [16], the authors study interference distribution in cognitive radio networks when interferers are distributed according to a Poisson point process, and thus assuming that transmitter locations are independent of each other. But, it has been shown e.g., [17] that spatial distribution of interferers plays an important role in interference distribution. Shape and variance of interference distribution do not depend only on the point process intensity, but is strongly linked to the spatial correlations between the points. For the same intensity of interferers, variance of interference may vary from 1 to 10 according to the considered point process [17], the worst variance being generated by the Poisson point process. In cognitive radio networks, secondary nodes use a sensing mechanism to avoid harmful interference to primary nodes. Moreover, secondary nodes detect signal/interference from the current transmissions of the other secondary nodes. Consequently, interferers are not distributed independently of each other, as with a Poisson point process, but the presence of a transmitter generates a spatial repulsion/inhibition area in its surrounding. In this paper, we propose point processes that aim to capture these correlations leading to a more accurate modeling of interference in cognitive radio networks.

We consider secondary nodes to monitor individual transmissions from primary nodes. Upon detecting no activities, they are allowed to transmit. In this paper, using concepts from stochastic geometry and the theory of point processes, we develop models for bounding the complementary cumulative distribution function (CCDF) of interference level from secondary nodes to a primary node. We consider a practical model which takes into account the MAC regulations and where the secondary Poisson process is judiciously thinned in two phases to avoid interference with the secondary as well as the primary nodes. The resulting process will be a modified version of the Matérn point process. We model the CCDF of interference level from secondary nodes to a primary node for this Matérn point process representing secondary nodes. Interference and throughput estimations for primary and secondary nodes are of interest. We use our obtained models to find the operation regions of the secondary network such that the interference constraint is satisfied on receiving primary nodes. We then obtain theoretical results on the primary and secondary throughputs and find the throughput limits under interference constraint.

The remainder of this paper is organized as follows. We describe the model, i.e., interference definition and the two point processes modeling primary and secondary interferers, in Section II. We present results on interference distribution for these point processes in Section III. Section IV considers the throughput under the interference constraint. Numerical evaluations and simulations are also provided to confirm the accuracy of the obtained results in Section V. Section VI concludes the paper.

II. MODEL

We focus on the interference level at a receiver located at the origin of the plane $O = (0, 0)$ and at a given time t. Interference is assumed to be the sum of signal strengths generated by all the interferers transmitting at time t. We use the following notations to denote interference from primary transmitters to a primary receiver ($I_{P\to P}$), from primary transmitters to a secondary receiver ($I_{P\to S}$), etc:

$$I_{P\to P} = \sum_{i=1}^{+\infty} P_P \xi_i l\left(\|Y_i\|\right) \text{ and } I_{S\to P} = \sum_{i=1}^{+\infty} P_S \zeta_i l\left(\|X_i\|\right), \tag{1}$$

$$I_{P\to S} = \sum_{i=1}^{+\infty} P_P \nu_i l\left(\|Y_i\|\right) \text{ and } I_{S\to S} = \sum_{i=1}^{+\infty} P_S \beta_i l\left(\|X_i\|\right) \tag{2}$$

where $\{\zeta_i\}$, $\{\xi_i\}$, $\{\nu_i\}$, and $\{\beta_i\}$ are independent and identically distributed random variables representing fading, $l\left(\|.\|\right)$ represents deterministic path loss (a decreasing function), P_P and P_S are the transmit power from primary and secondary nodes, and $(Y_i)_{i\in\mathbb{N}}$ (respectively $(X_i)_{i\in\mathbb{N}}$) represent locations of the interfering nodes in the primary (respectively in the secondary) network. We assume that fading is Rayleigh. Consequently, in the following we consider the random variables $\{\zeta_i\}$, $\{\xi_i\}$, $\{\nu_i\}$, and $\{\beta_i\}$ to be exponentially distributed with parameters equal to 1. For fading greater or lower than 1 in average, we can consider a lower (respectively greater) transmit power. In other words, the level of fading can be integrated in the transmitting power P_S or P_P.

It is obvious that according to (1) and (2), transmitter location plays a crucial role on interference. Interference distribution strongly depends on the spatial distribution of the simultaneous transmitters, i.e., $(X_i)_{i\in\mathbb{N}}$ and $(Y_i)_{i\in\mathbb{N}}$ distributions. Consequently, we consider two stationary point processes Φ_P ($\Phi_P = \{Y_i\}_{i\in\mathbb{N}}$) and Φ_S ($\Phi_S = (X_i)_{i\in\mathbb{N}}$) describing locations of the primary and the secondary nodes, respectively. Basically, a point process consists of a random sequence of points distributed in $\mathbb{R}^d$ (See [18] or [19] for details). In the two next subsections, we present the different point processes used to model transmitter locations.

A. Primary Nodes: Poisson

We consider Φ_P to be a Poisson point process distributed in $\mathbb{R}^2$ with intensity λ_P. A sample of this model is presented in Fig. 1(a). For this model, we have a cognitive radio system in the TV band in mind, where the primary nodes are TV transmitters. Therefore, primary node location does not depend on a sensing algorithm but more on the TV antennas deployment.

B. Secondary Nodes: A Modified Version of the Matérn Point Process

We assume that a secondary node listens to the medium before transmitting. If it detects the transmission of a frame from another secondary node or a primary node, it defers its own transmission. We assume that a transmission is detected by a node if the received signal strength from another node is greater

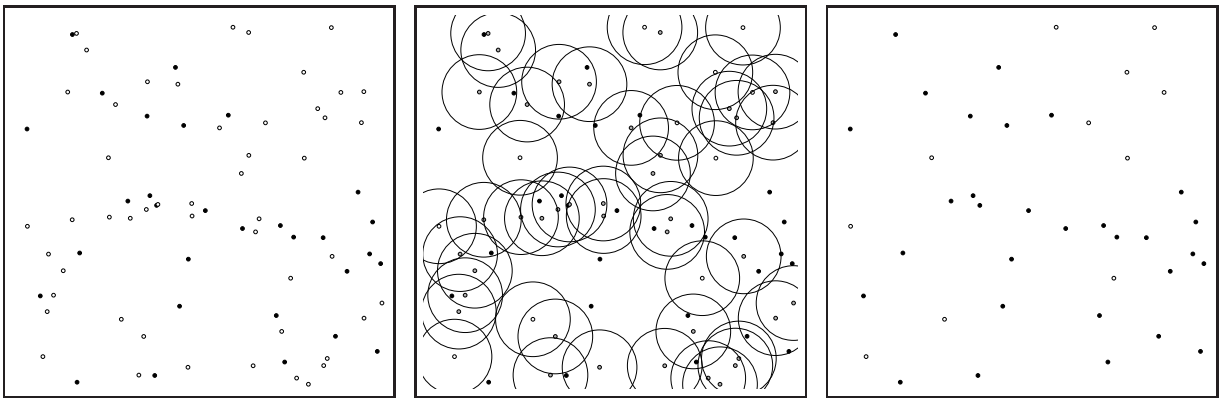

(a) (b) (c)

Fig. 1. Sample of the initial point processes and selection of the Secondaries: (a) Primary (black) and secondary nodes (white) are Poisson, (b) selection of the secondary nodes, and (c) primary and selected secondary nodes.

than a threshold γ. We also consider a simplified deterministic path loss and assume that the received signal strength is $P \cdot l(u)$ where u is the distance between the two nodes and P is the transmission power (P_P or P_S). For a given value of γ, there is therefore a maximal distance for which a transmission is detected. As this distance depends on the transmission power, we consider two different detection distances.

The Matérn point process is suitable to model the transmitter positions when using this medium access protocol. Basically, it is formed by removing a subset of the points of a Poisson point process in such a way that distances between all the pairs of remaining points are greater than a predefined constant (h_S or h_P in our case). This model has already been used to represent such networks in [20] and [21]. We propose a modified version of the Matérn point process in order to take into account detection from both primary and secondary nodes. We present below the classical Matérn point process, followed by a modified version which suits the context of our problem.

B.1 Definition of Matérn Process

We consider a homogeneous Poisson point process Φ with intensity λ. We associate with each point x a random variable $m(x)$ independently and uniformly distributed in $[0, 1]$. We perform a dependent thinning of the Poisson process. We retain a point x if and only if the points in the ball $b(x, h)$ contains no points with marks smaller than $m(x)$. Formally, the points of the Matérn is the set

$$\{x \in \Phi |\ m(x) < m(y),\ \ \forall y \in \Phi \cap b(x, h) \backslash x\}\,.$$

The intensity λ_h of this process is known (see for instance [18], page 164) and is given by:

$$\lambda_h = \frac{1 - \exp\left\{-\lambda \pi h^2\right\}}{\pi h^2}. \qquad (3)$$

B.2 Our Model

We use a modified version of the Matérn point process as the primary nodes do not apply the same rule to access the medium. The model is as follows:

- Simultaneous transmitters of the primary network are distributed according to a Poisson point process Φ_P with intensity λ_P.
- All the secondary nodes are distributed according to a Poisson point process Φ_S with intensity λ_S.
- We consider a classical Matérn point process with Φ_S as the underlying Poisson process and distance threshold h_S. It corresponds to a first thinning of Φ_S by taking into account transmission from secondary nodes.
- The Matérn point process is thinned a second time to take into account the transmission from the primary nodes. If a point of the Matérn is located at a distance less than h_P from a primary transmitter, it is removed.

The intensity of the selected secondary nodes denoted by $\lambda_S^{'}$ is then given by:

$$\lambda_S^{'} \quad = \quad \exp\left\{-\lambda_P \pi h_P^2\right\} \frac{1 - \exp\left\{-\lambda_S \pi h_S^2\right\}}{\pi h_S^2}. \qquad (4)$$

The computation of this intensity is straightforward. Intensity of the classical Matérn is known (given by (3)). The difference between the classical and the modified Matérn lies in the second step where a point (a secondary node) is removed if there is a point of the first Poisson point process (a primary node) at a distance less than h_P. A point selected after the first step will definitely be kept, if there is no point of Φ_P at a distance less than h_P. This event occurs with probability $\exp\left\{-\lambda_P \pi h_P^2\right\}$. Intensity of the modified Matérn point process is thus the Matérn intensity multiplied by the probability of having no primary node lying at distance less than h_P of a secondary node. A sample of this model and the way it is built is presented in Fig. 1:

- Fig. 1(a): Primary (black) and secondary nodes (white) are distributed according to two independent Poisson point processes.
- Fig. 1(b): Inhibition balls with radius h_S are plotted around the secondary nodes. Secondary nodes which are going to be removed (due to the two successive thinning) are in grey. The selected secondary nodes are white.
- Fig. 1(c): We keep only those secondary nodes which do not have primary nodes within their inhibition ball and satisfy the Matérn condition on the marks.

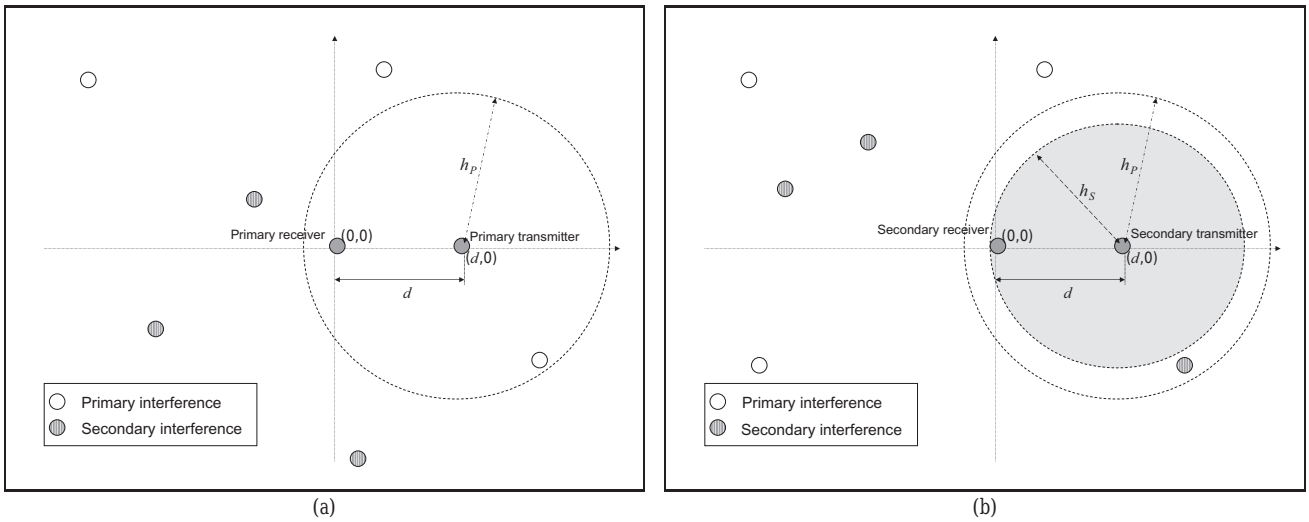

Fig. 2. Primary and secondary interferers distribution when we compute interference at a receiver: (a) A node at $(0,0)$ is receiving data from a primary transmitter at $D = (d,0)$. Primary interferers are distributed in $I\!R^2$ according to a Poisson point process. Secondary interferers are distributed according to a modified Matérn in $I\!R^2 \backslash b(D, h_P)$, (b) a node at $(0,0)$ is receiving data from a secondary transmitter at $D = (d,0)$. Primary interferers are distributed according to Poisson point process in $I\!R^2 \backslash b(D, h_P)$. Secondary interferers are distributed according to the modified Matérn in $I\!R^2 \backslash b(D, h_S)$.

C. Scenario

We consider two different cases for interference distributions. These are when the receiver 1) receives data from primary node and 2) receives data from secondary node. Computations differ for these two cases.

C.1 Interference at a Primary Receiver

We assume that the receiver is located at the origin of the plane and receives a frame from a primary transmitter located at $D = (d,0)$ (at distance d). Since this node is transmitting to the receiver, we do not take into account the signal strength from this transmitter in the interference computation. As primary nodes are distributed according to a Poisson point process, location of the other primary transmitters (the interferers) is still a Poisson point process (see Slyvniack's theorem in [18]). $I_{P\to P}$ is then the sum of the signal from primary transmitters. They are distributed as a Poisson point process in $I\!R^2$. But, secondary nodes are dependent on primary transmitters. According to our model, we cannot have a secondary node lying at a distance less than h_P from a primary node. Consequently, when we consider interference from secondary nodes, we shall assume that they are distributed in $I\!R^2 \backslash b(D, h_P)$ where $b(D, h_P)$ is a ball centered at D with radius h_P. $I_{S\to P}$ is then the sum of the signal from transmitters distributed as a modified Matérn point process in $I\!R^2 \backslash b(D, h_P)$. This scenario is shown in Fig. 2(a).

C.2 Interference at a Secondary Receiver

We assume that the receiver is located at the origin of the plane and receives a frame from a secondary transmitter located at $D = (d,0)$. We do not take into account the signal strength from this transmitter in the interference computation. As a primary transmitter cannot be at a distance less than h_P from a secondary transmitter, primary interferers follows a Poisson point process in $I\!R^2 \backslash b(D, h_P)$. $I_{P\to S}$ is the sum of the signal from transmitters distributed as a Poisson point process in $I\!R^2 \backslash b(D, h_P)$. Secondary nodes cannot lie at a distance less than h_S from each other. Therefore, when we consider interference from secondary nodes ($I_{S\to S}$) we shall assume that they are distributed as a modified Matérn point process in $I\!R^2 \backslash b(D, h_S)$. This scenario is shown in Fig. 2(b).

III. CCDF OF INTERFERENCE

In cognitive radio networks, secondary nodes must keep a low interference level in order to ensure that performance of the primary network is not deteriorated. The tolerable interference level can be expressed through different quantities. This allowance may be given through the probability that interference does not exceed a certain threshold:

$$P\left(I_{S\to P} > \eta\right) < \epsilon. \tag{5}$$

Conditions may also hold for the signal to interference plus noise ratio (SINR). This SINR can be evaluated for a primary receiver on the edge of the keep-out region or the protected region. Given a path-loss function, and a worst-case fading and noise, we can deduce the maximum interference from secondary nodes which ensures a SINR greater than this threshold. The admissible interference can also be deduced from the classical quantities used in cognitive radio literature [22], [23]: P_{MD} (probability of miss detection) and P_{FA} (probability of false alarm). Given a fixed protected region R_P, where secondary nodes are not supposed to be active, the probability of miss detection is the probability for a secondary node to detect the medium free whereas this node is within this protected region. This may happen when a secondary node estimates the energy in the targeted frequency band and compares it to a detection threshold [24], [25]. A very low signal level may be measured (due to a significant level of

fading for instance) whereas the node is in fact within the protected region. The false alarm probability is the opposite: This corresponds to the probability that the secondary node is outside the protected region whereas its sensing algorithm indicates that it is inside. These two probabilities are formally defined as follows. If $Detection = 0$ (respectively 1) when the sensing algorithm of the secondary node considers that it is outside (respectively inside) the protected region:

$$P_{MD} = P(Detection = 0 \mid \text{This node is in the protected region}),$$
$$P_{FA} = P(Detection = 1 \mid \text{This node is not in the protected region}).$$

The threshold used by the sensing algorithm at the secondary nodes to detect medium free/busy may be computed in order to keep these two probabilities under a certain value (0.1 for instance as in [22]). These quantities are generally computed taking into account only noise and fading [24], [25]. A more accurate computation should also involved interference from primary and secondary nodes. All these quantities (In (5), SINR, P_{MD} or P_{FA}) require the knowledge of the interference distribution, in particular the CCDF. For the proposed models, we develop bounds and approximations on these probabilities to determine the parameters for the secondary network for which conditions on interference on the primary network is met. CCDF for $I_{P\to P}$ and $I_{S\to P}$ are presented in subsection III-A and III-B, from which we deduce P_{MD} and P_{FA} in subsection III-C.

A. Interference Generated by the Primary Nodes (Poisson)

We propose a lower bound on the CDF of the interference generated by the primary nodes ($I_{P\to P}$ and $I_{P\to S}$). We then deduce an upper bound on the CCDF. We also propose an approximation which is easier to compute than this bound.

Proposition 1: The lower bound of $I_{P\to P}$ is:

$$P\left(I_{P\to P}\le\eta\right) \ge 1-2\pi\lambda_P\int_0^{+\infty}\exp\left\{-\frac{\eta}{P_P l(r)}\right\}\exp\Bigg\{ - \lambda_P 2\pi\int_r^{+\infty}\left(1-\frac{1-\exp\left\{-\frac{\eta}{P_P}\left(\frac{1}{l(w)}-\frac{1}{l(r)}\right)\right\}}{1-\frac{l(w)}{l(r)}}\right)w dw\Bigg\} r dr. \tag{6}$$

The upper bound on the CCDF is then:

$$P\left(I_{P\to P}\ge\eta\right) \le 2\pi\lambda_P\int_0^{+\infty}\exp\left\{-\frac{\eta}{P_P l(r)}\right\}\exp\Bigg\{ - \lambda_P 2\pi\int_r^{+\infty}\left(1-\frac{1-\exp\left\{-\frac{\eta}{P_P}\left(\frac{1}{l(w)}-\frac{1}{l(r)}\right)\right\}}{1-\frac{l(w)}{l(r)}}\right)w dw\Bigg\} r dr. \tag{7}$$

For $I_{P\to S}$, we obtain

$$P\left(I_{P\to S}\ge\eta\right) \le \lambda_P\int_{\mathbb{R}^2\setminus b(D,h_P)}\exp\left\{-\frac{\eta}{P_P l(\|x\|)}\right\} \times\exp\Bigg\{ - \lambda_P\int_{\|u\|>\|x\|;\|u-D\|>h_P}\left(1 - \frac{1-\exp\left\{-\frac{\eta}{P_P}\left(\frac{1}{l(\|u\|)}-\frac{1}{l(\|x\|)}\right)\right\}}{1-\frac{l(\|u\|)}{l(\|x\|)}}\right)du\Bigg\} x dx. \tag{8}$$

The proof is given in the Appendix. The approximation used to evaluate the CCDF of $I_{P\to P}$ is found by taking the second integral of (7) equal to 0. It is a good approximation when η or λ_P is small:

$$P\left(I_{P\to P}\ge\eta\right) \approx 2\pi\lambda_P\int_0^{+\infty}\exp\left\{-\frac{\eta}{P_P l(r)}\right\} r dr, \tag{9}$$

$$P\left(I_{P\to S}\ge\eta\right) \approx \lambda_P\int_{\mathbb{R}^2\setminus b(D,h_P)}\exp\left\{-\frac{\eta}{P_P l(\|x\|)}\right\} dx. \tag{10}$$

B. Interference Generated by the Secondary Nodes (Modified Matern)

We consider the modified version of the Matérn point process to model the secondary nodes (presented in subsection II-B). We compute interference for a node located at the origin of the plane $O=(0,0)$. This node receives data from a transmitter located at $D=(d,0)$. As explained in subsection II-C, there is an inhibition ball centered at D. This ball is $b(D,h_P)$ when the transmitter at D is a primary node, and $b(D,h_S)$ otherwise. From the intensity of the modified Matérn (see (4)), it is easy to find an upper bound on the interference generated by the secondary nodes. It is found by using the Markov inequality:

$$P\left(I_{S\to P}>\eta\right) \le \frac{E\left[I_{S\to P}\right]}{\eta}. \tag{11}$$

Since the modified Matérn is stationary, we can apply Campbell formula (see [18] page 104) to compute mean interference (with $\lambda_S^{'}$ given by (4)):

$$E\left[I_{S\to P}\right] = \lambda_S^{'}P_S\int_{\mathbb{R}^2\setminus\overline{b(D,h_P)}} l\left(\|u\|\right)du, \tag{12}$$

$$E\left[I_{S\to S}\right] = \lambda_S^{'}P_S\int_{\mathbb{R}^2\setminus\overline{b(D,h_S)}} l\left(\|u\|\right)du. \tag{13}$$

The bound given by (11) being not tight, we propose an approximation to compute this CCDF instead. It has been shown through a statistical study of interference [17], that interference generated by a Matérn point process follows a log-normal distribution. In order to determine the two parameters of this distribution, we use mean and variance of interference. The mean interference is given by (12). The second moment of interference generated by a Matérn point process has been computed in [26]. We obtain a variant of this second moment for our model. Let us define $\nu(A)$ the Lebesgue measure of A (area of A) for $A\subset\mathbb{R}^2$. We have:

$$E\left[I_{S\to P}^2\right] = \lambda_S^{'} \int_{I\!R^2\setminus b(D,h_P)} P_S^2 E\left[\zeta^2\right] l(\|x\|)^2 dx + \frac{2P_S^2}{\pi h_S^2} \int_{I\!R^2\setminus b(D,h_P)} \int_{I\!R^2\setminus (b(x,h_S)\cup b(D,h_P))} E[\zeta_1\zeta_2] \times \left[\frac{1-\exp\{-\lambda_S \nu(b(x,h_S)\cup b(y,h_S))\}}{\nu(b(x,h_S)\cup b(y,h_S))} - \frac{\exp\left\{-\lambda_S \pi h_S^2\right\} - \exp\{-\lambda_S \nu(b(x,h_S)\cup b(y,h_S))\}}{\nu(b(x,h_S)\cup b(y,h_S)) - \pi h_s^2} \right] \times \exp\{-\lambda_P \nu(b(x,h_P)\cup b(y,h_P))\} l\left(\|x\|\right) l\left(\|y\|\right) dydx \tag{14}$$

with $E[\zeta^2] = 2$ and $E[\zeta_1\zeta_2] = 1$. The proof is straightforward with regard to the one presented in Proposition 3 of [26]. It suffices to weight the probability for two points to belong to the Matérn point process by the probability of having no point of Φ_P (a primary node) at a distance less than h_P (from these two points). In the equation above, this probability is included in $\lambda_S^{'}$ for the first term, and is equal to $\exp\{-\lambda_P \nu(b(x,h_P)\cup b(y,h_P))\}$ for the second term. The approximation is then $I_{S\to P} \rightsquigarrow \text{log-normal}(m,\sigma^2)$ where m and σ^2 correspond to mean and variance of this log-normal distribution: m is given by (12) and $\sigma^2 = E\left[I_{S\to P}^2\right] - m^2$ with $E\left[I_{S\to P}^2\right]$ given by (14).

For $I_{S\to S}$, we use the same approximation. Parameters of the log-normal distribution are given by (13) for the mean and (14) for $E\left[I_{S\to S}^2\right]$ where we have to substitute $b(D,h_P)$ by $b(D,h_S)$.

C. Probability of Miss Detection and False Alarm

In order to compare the classical P_{FA} and P_{MD} probabilities with and without interference considerations, we propose an analytical derivation of these two quantities. We assume that the protected region is a ball centered at a primary transmitter located at $D = (d,0)$ and with radius R_P. R_P will be equal to h_p (the inhibition radius around the primary nodes) in all our numerical evaluations. A secondary node, located at the origin, senses the medium to determine if it is in the protected region or not. The decision is made by comparing the sensed energy level with a specific threshold γ. The received signal strength at this secondary node can be estimated as the sum of interference from primary and secondary nodes, plus noise, plus the signal strength from the primary transmitter. Interference at the sensing node is the same as interference at a primary node described in subsection II-C.1. Consequently, interference at the sensing node is denoted as $I_{P\to P} + I_{S\to P}$ in the next formulas.

P_{MD} is the probability that the signal strength is less than γ whereas $d < R_P$ and P_{FA} is the probability that it is greater than γ whereas $d \geq R_P$. In the following equations, we will assume that the noise W is constant. To obtain formula with a random noise, it suffices to condition the final results with the distribution of W. We obtain,

$$P_{MD} = P\left(I_{S\to P} + I_{P\to P} + P_P \xi l(d) + W < \gamma\right) \text{ with } d < R_P, \tag{15}$$

$$P_{FA} = P\left(I_{S\to P} + I_{P\to P} + P_P \xi l(d) + W > \gamma\right) \text{ with } d \geq R_P. \tag{16}$$

For a constant noise W, we obtain:

$$\begin{aligned} P_{MD} &= P\left(I_{S\to P} + I_{P\to P} + P_P \xi l(d) + W < \gamma\right) \\ &= P\left(I_{P\to P} < \gamma - W - I_{S\to P} - P_P \xi l(d)\right) \\ &= \int_0^{\frac{\gamma-W}{P_P l(d)}} \int_0^{\gamma - W - P_P u l(d)} P\left(I_{P\to P} < \gamma - W - s - P_P u l(d)\right) \\ &\quad f_{LogN}(s)ds \exp\{-u\}du. \end{aligned} \tag{17}$$

The last equation has been obtained by conditioning by the distribution of ξ and $I_{S\to P}$ for which we assume that it follows a log-normal distribution. $f_{LogN}(.)$ is the pdf of this log-normal distribution. The two parameters μ and σ of this distribution can be computed from mean and variance of $I_{S\to P}$ ($E[I_{S\to P}] = \exp\{\mu + \frac{\sigma^2}{2}\}$ and $Variance(I_{S\to P}) = (\exp\{\sigma^2\} - 1)\exp\{2\mu + \sigma^2\}$). Mean and variance are given by (12) and (14) from which we deduce the two parameters σ and μ. A random noise can also be considered, it adds an integral function of the noise distribution in the formula above. $P(I_{P\to P} < \gamma - W - I_{S\to P} - P_P u l(d))$ is estimated from (6). Also, we assumed that $I_{P\to P}$ and $I_{S\to P}$ are independent.

Generally, computations of these probabilities neglect interference from primary nodes. It simplifies this equation (with $I_{P\to P} = 0$):

$$\begin{aligned} P_{MD} &= P\left(I_{S\to P} + P_P \xi l(d) + W < \gamma\right) \\ &= P\left(I_{S\to P} < \gamma - W - P_P \xi l(d)\right). \end{aligned} \tag{18}$$

If we condition by ξ and assume that W is constant (with $\gamma > W$), we obtain:

$$\begin{aligned} P_{MD} &= \int_0^{\frac{\gamma-W}{P_P l(d)}} P\left(I_{S\to P} < \gamma - W - P_P u l(d)\right) \exp\{-u\}du \\ &= \int_0^{\frac{\gamma-W}{P_P l(d)}} \frac{1}{2} erfc\left(-\frac{\ln(\gamma - W - P_P u l(d)) - \mu}{2\sigma}\right) \\ &\quad \times \exp\{-u\}du. \end{aligned} \tag{19}$$

Computations of P_{FA} is the same. It suffices to take $P_{FA} = 1 - P_{MD}$ but with $d \geq R_P$.

IV. THROUGHPUT ESTIMATION

In this section, we focus on the obtainable throughput by both primary and secondary networks. This throughput is defined as the mean number of frames that are correctly received per second in a unit square area. We estimate the throughput as follows:

$$T = \lambda(1 - FER)\frac{1}{t_f} \tag{20}$$

where λ is the intensity of the simultaneous transmitters, t_f is the mean time required to send a frame, and FER is the frame error rate. We compute this quantity for the model that we have

developed: primary nodes are distributed according to a Poisson point process and secondary nodes are distributed according to our modified Matérn process. For the *FER* we use the definition and method developed in [20]:

$$FER \quad = \quad P\left(SINR < \theta\right). \tag{21}$$

In the proposition below, we give the throughput for the primary and secondary networks. We consider the *FER* for a node which is located at the origin and is receiving a frame from a node at distance d. It corresponds to scenarios described in subsections II-C.1 and II-C.2 where the transmitting node at D is a primary node (respectively secondary node). First, we find the *FER* for the modified Matérn point process. We consider FER for a transmission from a primary node. Computations for the secondary network is equivalent. Then, we deduce the throughput from (20). We assume that the noise is an independent random variable W. Let ξ an exponential random variable with parameter 1, we get:

$$\begin{aligned} FER = P\left(SINR < \theta\right) &= P\left(\frac{P_P \xi l(d)}{W + I_{S\to P} + I_{P\to P}} < \theta\right) \\ &= P\left(\xi < \frac{\theta(I_{P\to P} + I_{S\to P} + W)}{P_P l(d)}\right) \\ &= 1 - E\left[\exp\left\{-\frac{\theta}{P_P l(d)} I_{S\to P}\right\} \exp\left\{-\frac{\theta}{P_P l(d)} I_{P\to P}\right\}\right] \\ &\times E\left[\exp\left\{-\frac{\theta}{P_P l(d)} W\right\}\right]. \end{aligned} \tag{22}$$

It is not possible to compute this quantity analytically as $I_{P\to P}$ and $I_{S\to P}$ are dependent and the joint distribution is unknown. As an approximation, we assume that $I_{S\to P}$ and $I_{P\to P}$ are independent. We will show through simulations that this assumption does not bias the results. Using this assumption, we obtain:

$$\begin{aligned} FER = 1 &- E\left[\exp\left\{-\frac{\theta}{P_P l(d)} I_{S\to P}\right\}\right] \\ &\times E\left[\exp\left\{-\frac{\theta}{P_P l(d)} I_{P\to P}\right\}\right] E\left[\exp\left\{-\frac{\theta}{P_P l(d)} W\right\}\right]. \end{aligned} \tag{23}$$

FER can thus be expressed with regard to the Laplace transforms of W, $I_{S\to P}$ and $I_{P\to P}$. We have shown that $I_{S\to P}$ can be approximated by a log-normal distribution, so we use the Laplace transform of the log-normal distribution to compute $E\left[\exp\left\{-\theta I_{S\to P}/P_P l(d)\right\}\right]$. Laplace transform of the noise is also directly computable from its distribution. The expression for $I_{P\to P}$ is given in the proof of Proposition 2.

Proposition 2: Approximation of throughputs for primary and secondary networks are:

$$\begin{aligned} T_{\text{primary}} = \lambda_P \exp&\left\{-\lambda_P 2\pi \int_0^{+\infty} \frac{\theta l(r)}{l(d) + \theta l(r)} r dr\right\} \\ &\times E\left[\exp\left\{-\frac{\theta}{P_P l(d)} I_{S\to P}\right\}\right] E\left[\exp\left\{-\frac{\theta}{P_P l(d)} W\right\}\right] \frac{1}{t_f}, \end{aligned} \tag{24}$$

$$\begin{aligned} T_{\text{secondary}} = \lambda_S^{'} \exp&\left\{-\lambda_P \int_{\mathbb{R}^2 \setminus b(D,h_p)} \frac{\theta P_P l(|x|)}{P_S l(d) + \theta P_P l(|x|)} dx\right\} \\ &\times E\left[\exp\left\{-\frac{\theta}{P_S l(d)} I_{S\to S}\right\}\right] E\left[\exp\left\{-\frac{\theta}{P_S l(d)} W\right\}\right] \frac{1}{t_f}. \end{aligned} \tag{25}$$

where $\lambda_S^{'}$ is the intensity of the Matérn point process given by (4) and where $I_{S\to P}$ is supposed to follow a log-normal distribution with mean and variance given by (12) and (14). In (12) and (14), $b(D_P, h_P)$ must be replaced by $b(D_S, h_S)$ in the first integral when we consider the FER for the secondary nodes. In order to obtain the FER in the secondary network, it suffices to substitute $P_P l(d)$ by $P_S l(d)$ in (22).
The proof is given in the Appendix.

V. NUMERICAL EVALUATIONS AND SIMULATIONS

In this section, we present the simulation results. We implemented a simulator coded in C. This software simulates the cognitive radio network: Poisson for the primary nodes and the modified Matérn for secondary nodes. It aims to estimate the accuracy of approximations we made: Log-normal distribution for $I_{S\to P}$ and the independence between $I_{S\to P}$ and $I_{P\to P}$. Also, it is used to compare the performances of the cognitive radio network when interference is taken into account with a scenario without interference.

We consider two different contexts of applications for cognitive radio. Scenarios and results for these two contexts are presented in the two next sections.

A. Cognitive Radio in the Television Bands

We consider the classical scenario targeted by the IEEE 802.22 standard [27]. It describes cognitive radio to operate in the television bands. It allows a secondary node to opportunistically access the TV bands. The sensing algorithm used by secondary nodes to detect an activity on this license band and its associated parameters is thus crucial to guarantee the absence of a television signal and maximize the usage of this spectrum. This problem has already been addressed in [22] and [24], but all these studies do not take into account interference level from secondary nodes in the sensing algorithm. For this scenario, we show the impact of interference from secondary nodes on the dimensioning of IEEE 802.22 sensing algorithm. The simulation parameters are similar to the ones used in [22] and [24]. We assume that a TV station is transmitting at $1\ MW$ ($90\,dBm$) in the UHF at $615\ MHz$. We consider the path-loss function and shadowing model proposed in the ITU-R 1546 recommendation [28]. The path-loss function plotted in Fig. 3 is a continuous piecewise polynomial function. The exponent parameters is 3 for distance d less than $1\,km$, 2.7 for $d \leq 30\,km$, 7.65 for $d \leq 100\,km$, and 8.38 for greater distances. The transmitting power for secondary nodes is $36\,dBm$. It corresponds to the maximum power allowed by the IEEE 802.22 standard. The distance between the TV antenna and the primary receiver for which we compute SNR and SINR is $134.2\,km$. This distance equals to the protection contour computed in [22] and [24]. It corresponds to the distance at which all TV receivers not receive harmful interference (it only takes into account noise, and

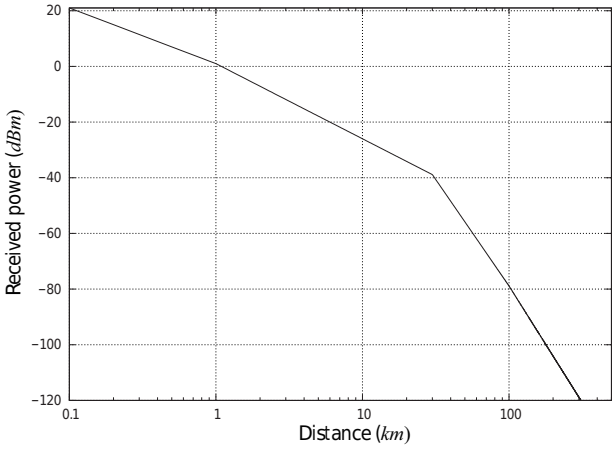

Fig. 3. Path-loss function.

guarantees that the ratio between received signal and noise is at least $23\,dB$). Standard deviation of the fading is equal to $5.5\,dB$. It has been set according to the ITU-R 1546 recommendation. Values of h_S and h_P correspond to the distance at which the signal from a secondary (respectively primary) node is equal to $-116\,dBm$. It is the threshold given in the IEEE 802.22 standard. We chose a very small intensity for the primary nodes, because interference from primary to primary nodes was considered more or less negligible, at least compare to secondary interference. Indeed, TV antennas has been planned in order to keep a low level of interference between them. Instead, we wanted to highlight the impact of interference from secondary nodes (for which there are 10,000 potential transmitters: 1 for $10 \times 10\ km^2$) on primary communications. The other parameters are given in Table 1.

A.1 Interference Distribution

In Figs. 4(a) and 4(b), we plotted interference CCDF at a primary receiver where interference is generated by primary and secondary nodes. The theoretical curves correspond to (7) and (9) in Fig. 4(a). In Fig. 4(b), we plotted interference distribution generated by secondary nodes ($I_{S\to P}$). It compares simulations to the approximation based on a log-normal distribution where parameters are set according to mean and variance of $I_{S\to P}$. It appears that the different assumptions made in the model do not impact the results, and the proposed theoretical distribution of interference matches perfectly to the simulated ones.

A.2 SNR and SINR Distributions

In Fig. 5 we plotted the CCDF of SNR and SINR for the primary receiver. The CCDF of SINR is given by (22), and the SNR is not given here but it is trivial as this quantity depends only on the fading distribution (the noise was assumed constant for these simulations). Simulations fit perfectly well to the theoretical curves. Also, we observe that there is significant difference between SNR and SINR distributions. Therefore, it proves that the dimensioning of the sensing algorithm cannot just take into account the SNR, but has to consider interference.

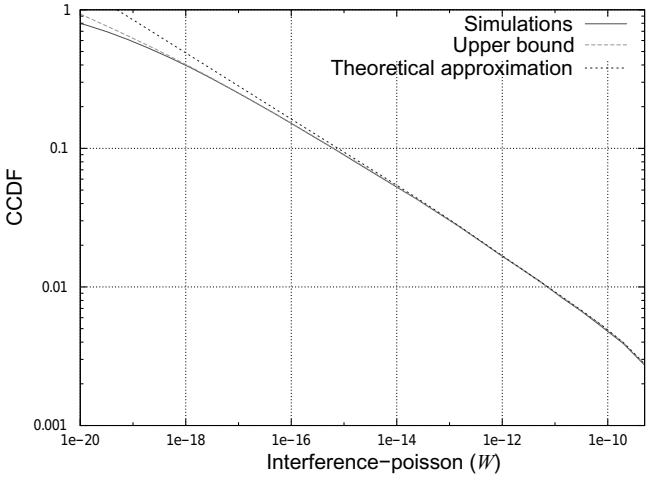

(a)

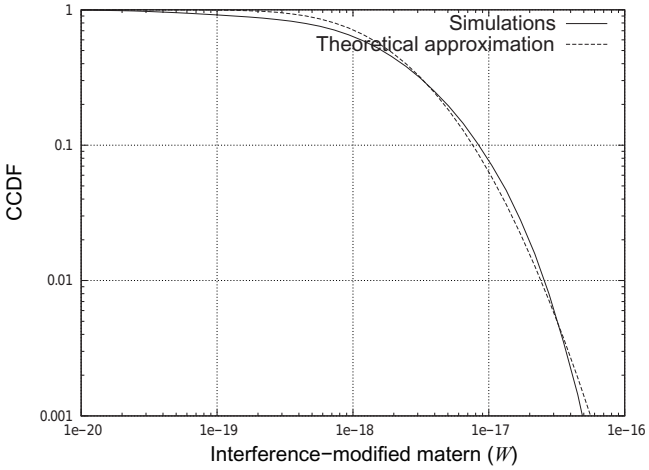

(b)

Fig. 4. CCDF of $I_{P\to P}$ and $I_{S\to P}$. Comparison between theoretical results and simulations: (a) CCDF of $I_{P\to P}$ for the Poisson point process and the upper bound and (b) CCDF of $I_{S\to P}$ for the modified Matérn point process and the approximation from log-normal.

A.3 Probability of False Alarm and Miss Detection

In order to evaluate the impact of interference on performances, we consider the two classical quantities P_{FA} and P_{MD} as presented in subsection III-C. Theoretical curves are computed according to (19) and its complementary ($P_{FA} = 1 - P_{MD}$). The threshold γ is set to $-93.12\,dBm$. It corresponds to the signal strength from the TV transmitter on the protection contour (at $134.2\ km$) without considering noise and interference. h_S and h_P are set accordingly ($h_S = 22.3\ km$, $h_P = 134.2\,km$).

In Fig. 6(a), we plotted the probability P_{MD} with regard to the distance between the primary receiver and the TV transmitter. It gives the probability for a secondary node to miss the detection of the TV transmitter. The limit of the protected region is represented with a vertical line at $134.2\ km$. In order to compare to the classical approach where only noise and fading is considered, we plotted this probability without interference (*Simulations - without interference* in the figure). We observe that all the curves fit until $100\ km$, then interference from sec-

Simulation parameters	Numerical values
Emission Power for primary nodes	$90\ dBm$
Emission Power for secondary nodes	$36\ dBm$
Standard deviation of fading	$5.5\ dB$
primary intensity (λ_P)	$1.27e^{-6}$ (1 node in $500 \times 500\ km^2$ in average)
secondary intensity (λ_S)	0.003183 (1 node in $10 \times 10\ km^2$ in average)
Distance between the primary receiver and its transmitter	$134.2\ km$ ($D = (134.2, 0.0)$)
Inhibition ball between primary and secondary nodes (h_P)	$236\ km$
Inhibition ball between secondary and secondary nodes (h_S)	$50\ km$
Noise	$-99.2\ dBm$
Observation window	$1,000 \times 1,000\ km^2$
Number of samples	$200,000$

Table 1. Simulation parameters for the IEEE 802.22 scenario.

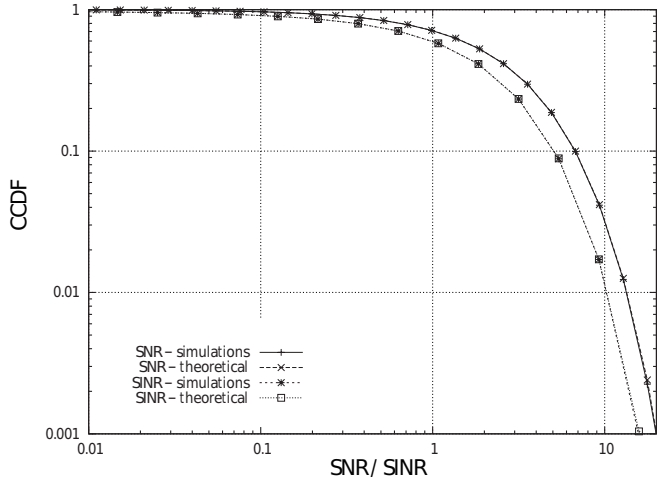

Fig. 5. CCDF of SNR and SINR.

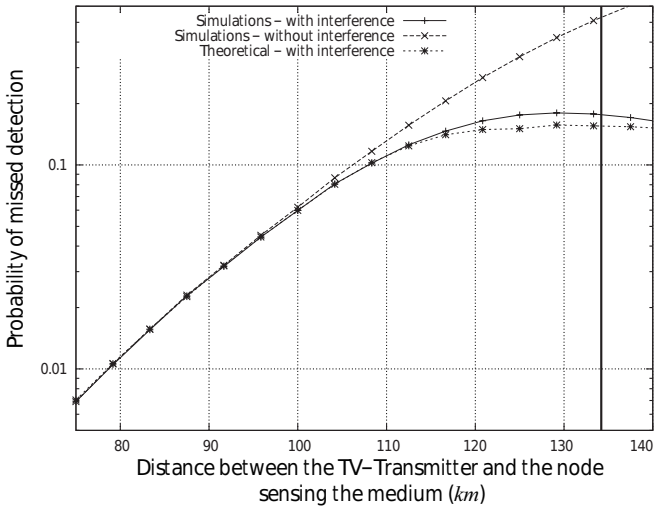

(a)

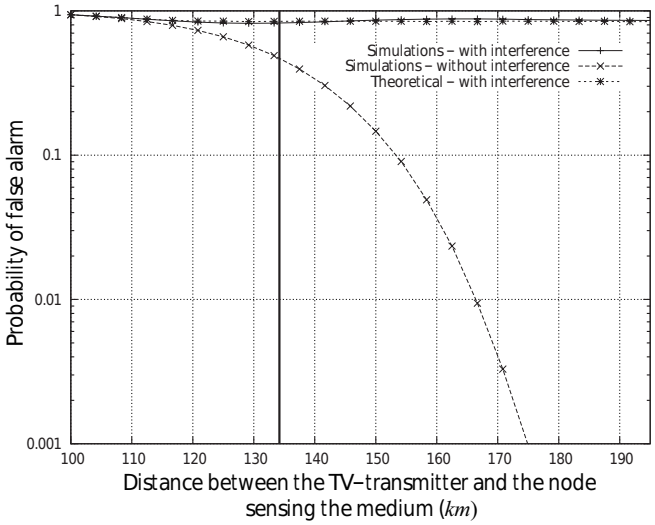

(b)

Fig. 6. Probability of miss detection and false alarm: (a) Probability of miss detection and (b) probability of false alarm.

ondary nodes increases the energy level in the TV band making the detection easier. For the chosen parameters, there is significant difference for the values of P_{MD} with and without interference. For the probability of false alarm plotted in Fig. 6(b), results have to be considered for distance greater than $134.2\ km$. For these distances, interference from secondary nodes is often above the detection threshold leading to a greater P_{FA} with regard to the case where interference is not taken into account. Therefore, secondary nodes detect a busy medium. However, it cannot be considered as a false alarm as the medium is used by secondary nodes. The computation of P_{FA} with interference is thus questionable.

B. Data Network

In this second scenario we consider a more original network (with respect to the cognitive radio literature). We wanted to estimate the gain of cognitive radio in a wireless data networks. We assume that a frequency band has been licensed for a wireless data network. Primary nodes use this frequency band to exchange frames in an asynchronous manner. Secondary nodes can use this band without disturbing primary transmissions. Secondary nodes behave as in the previous scenario. They sense the medium to evaluate the energy and transmit a frame if this energy is below a predefined threshold. The theoretical model is the same, only the parameters change. They are given in Table 2, and are close to the one used in wireless data network (IEEE 802.11a to be precise). We focus on the throughput of primary

Simulation parameters	Numerical values
Path-loss function	$l(u) = \min(1, (\beta/4\pi u)^{\alpha})$
β	0.346 m (wavelength)
α	3.0
Emission power for primary nodes	$40\ mW$
Emission power for secondary nodes	$40\ mW$
Primary intensity (λ_P)	0.00005 (1 node in $140 \times 140\ m^2$ in average)
Secondary intensity (λ_S)	0.001 (1 node in $33 \times 33\ m^2$ in average)
Inhibition ball between primary and secondary nodes (h_P)	$50\ m$
Inhibition ball between secondary and secondary nodes (h_S)	$50\ m$
Observation window	$100 \times 100\ km^2$
Number of samples	$1,000,000$

Table 2. Simulation parameters for the data network.

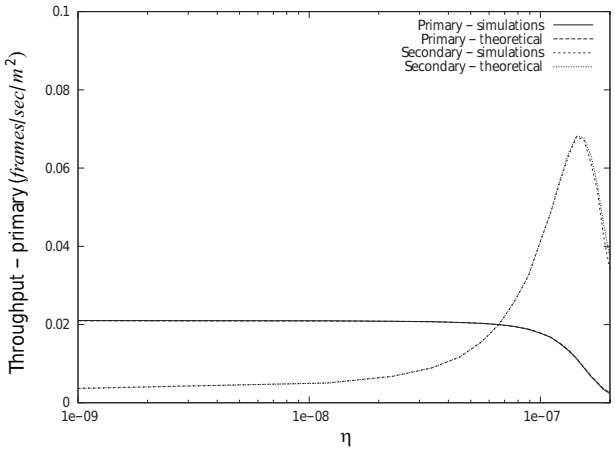

Fig. 7. Throughput in the data network.

and secondary networks. We want to determine the best thresholds (ϵ, η) on the condition on interference given by (5) which maximizes secondary throughput without impacting throughput in the primary network.

For a given value of ϵ, we use the bound and approximation developed in Section III to determine parameters of the secondary network in such a way that transmissions from secondary nodes satisfy the condition on interference. In Fig. 7, we vary η of (5) and we observe the throughput under this constraint. For this figure, the path-loss is $l(u) = \min\left(\left(\frac{\beta}{4\pi u}\right)^{\alpha}, 1\right)$ with $\beta = 0.346\ m$ (wavelength) and $\alpha = 3$. The other parameters are $\lambda_P = 0.00005$, $\lambda_S = 0.001$, $P_S = P_P = 40\ mW$, and $\theta = 10$. The distance between receiver and transmitter is $d = 10$ meters. h_S and h_P are computed according to the method described in subsections III-A and III-B. $\epsilon = 5.0e-02$. η varies (η and ϵ are defined in (5)). We considered $5,000$ samples. We also performed simulations varying ϵ rather than η. It led to the same behavior, and is consequently not shown in this paper. In this figure, we can observe that throughput of the secondary network forms a peak. This peak is due to the following phenomena. When η increases, the intensity of the simultaneous secondary transmitters increases, since the interference constraint becomes looser. There are, therefore, more transmitters and more frames received. When this intensity becomes high, interference generated by secondary nodes becomes significant increasing the *FER* and decreasing the throughput. Throughput of the primary network is more regular. It is not impacted by secondary node transmissions until η reaches a threshold (approximately $\eta = 6.0e^{-8}$). For this model, η (and consequently γ, h_S, and h_P) should be chosen close to this threshold. It offers a good throughput to the secondary network without penalizing throughput of the primary network.

A consistent technique to compute the thresholds (η, ϵ) is to set a tolerable reduction of primary throughput due to secondary interference. The pair (η, ϵ) can be computed in such a way that the primary throughput ratio (throughput with interference over throughput without interference) is greater than a predefined threshold. This ratio is easily computable. It suffices to compute the throughput given by (24) in Proposition 2 to consider the throughput with secondary interference, and the same formula with $I_{S\to P} = 0$ to obtain the throughput without interference. Unfortunately, these equations cannot be handled to obtain a closed form for (η, ϵ), and a numerical calculation must be performed.

VI. CONCLUSION

Obtaining interference distribution and throughput for primary and secondary nodes in a cognitive radio network is of considerable interest. We proposed a modified version of the Matérn point process to model accurately interferer locations. Our model takes into account the spatial correlation between primary and secondary nodes, as well as between secondary nodes. This spatial correlation models the sensing mechanism performed by the secondary nodes to detect transmission in progress from primary or secondary nodes. We derived closed formulas and bounds for the interference distribution and throughputs for both primary and secondary networks. Numerical results show that interference plays an important role on the cognitive radio network performance. In particular, the probability of miss detection is overestimated when interference is not taken into account, whereas probability of false alarm is underestimated. Thus, accurate interference distribution is required to estimate properly the different threshold used by the secondary nodes to decide if they can transmit without disturbing primary communications. We have also shown that secondary nodes may

have a considerable throughput without penalizing primary performances. The proposed analytical formulas for throughput and interference can be used to obtain operational secondaries parameters. They can be optimized to generate a low level of interference on primary nodes leading to a negligible increase on FER, or equivalently a negligible reduction of throughput, whereas optimizing throughput of the secondary network.

Appendix

Proof: Proof of Proposition 1. We distinguish two cases *a)* the bound on $I_{P\to P}$, and *b)* the bound on $I_{P\to S}$.

Bound on $I_{P\to P}$. First, we compute the bound for $I_{P\to P}$ where the points are distributed according to a Poisson point process with intensity λ_P. The points of this point process are denoted $(Y_i)_{i>0}$ with $\|Y_i\| \geq \|Y_j\|$ if $i > j$. The lower bound is computed as follows:

$$P\left(I_{P\to P} \leq \eta\right) \tag{26}$$

$$= P\left(P_P \xi_1 l\left(\|Y_1\|\right) \leq \eta - \sum_{i=2}^{+\infty} P_P \xi_i l\left(\|Y_i\|\right)\right) \tag{27}$$

$$= P\left(\xi_1 \leq \frac{\eta - \sum_{i=2}^{+\infty} P_P \xi_i l\left(\|Y_i\|\right)}{P_P l\left(\|Y_1\|\right)}\right) \tag{28}$$

$$= E\Bigg[\left(1 - \exp\left\{-\frac{\eta - \sum_{i=2}^{+\infty} P_P \xi_i l\left(\|Y_i\|\right)}{P_P l\left(\|Y_1\|\right)}\right\}\right) \tag{29}$$

$$\times \mathbb{1}_{\eta - \sum_{i=2}^{+\infty} P_P \xi_i l(\|Y_i\|) > 0} + \mathbb{1}_{\eta - \sum_{i=2}^{+\infty} P_P \xi_i l(\|Y_i\|) \leq 0}\Bigg]. \tag{30}$$

We set,

$$I^k_{P\to P} = \sum_{i=k}^{+\infty} P_P \xi_i l\left(\|Y_i\|\right). \tag{31}$$

$$P\left(I_{P\to P} \leq \eta\right) \tag{32}$$

$$= P\left(I^2_{P\to P} \leq \eta\right) - E\left[\exp\left\{-\frac{\eta - I^2_{P\to P}}{P_P l\left(\|Y_1\|\right)}\right\}\mathbb{1}_{I^2_{P\to P}<\eta}\right]$$

$$= P\left(\xi_2 \leq \frac{\eta - I^3_{P\to P}}{P_P l\left(\|Y_2\|\right)}\right) - E\left[\exp\left\{-\frac{\eta - I^2_{P\to P}}{P_P l\left(\|Y_1\|\right)}\right\}\mathbb{1}_{I^2_{P\to P}<\eta}\right] \tag{33}$$

$$= P\left(I^3_{P\to P} \leq \eta\right) - \sum_{k=1}^{2} E\left[\exp\left\{-\frac{\eta - I^{k+1}_{P\to P}}{P_P l\left(\|Y_k\|\right)}\right\}\mathbb{1}_{I^{k+1}_{P\to P}<\eta}\right]. \tag{34}$$

By recurrence, we obtain for $n > 1$:

$$P\left(I_{P\to P} \leq \eta\right) = P\left(I^n_{P\to P} \leq \eta\right) - \sum_{k=1}^{n-1} E\left[\exp\left\{-\frac{\eta - I^{k+1}_{S\to P}}{P_P l\left(\|Y_k\|\right)}\right\}\mathbb{1}_{I^{k+1}_{P\to P}<\eta}\right] \tag{35}$$

and when $n \to +\infty$,

$$P\left(I_{P\to P} \leq \eta\right) = 1 - \sum_{k=1}^{+\infty} E\left[\exp\left\{-\frac{\eta - I^{k+1}_{P\to P}}{P_P l\left(\|Y_k\|\right)}\right\}\mathbb{1}_{I^{k+1}_{P\to P}<\eta}\right]. \tag{36}$$

We apply the Campbell formula [18]:

$$P\left(I_{P\to P} \leq \eta\right) = 1 - \lambda_P \int_{\mathbb{R}^2} E^0\left[\exp\left\{-\frac{\eta - I^x_{P\to P}}{P_P l\left(\|x\|\right)}\right\}\mathbb{1}_{I^x_{P\to P}<\eta}\right] dx \tag{37}$$

where $E^0[.]$ is the expectation under Palm measure [18], [29] and

$$I^x_{P\to P} = \sum_{Y_i \in \mathbb{R}^2 \setminus \overline{b(-x,\|x\|)}}^{+\infty} P_P \xi_i l\left(\|Y_i\|\right) \tag{38}$$

where $b(-x, \|x\|)$ is the ball centered at $-x$ with radius $\|x\|$ and $\overline{A}$ is the closed set of A.

As the Poisson point process is stationary, we can use the following definition instead:

$$I^x_{P\to P} = \sum_{Y_i \in \mathbb{R}^2 \setminus \overline{b(0,\|x\|)}}^{+\infty} P_P \xi_i l\left(\|Y_i\|\right). \tag{39}$$

Moreover, from the Slivnyak's theorem [18], we have:

$$E^0\left[\exp\left\{-\frac{\eta - I^x_{P\to P}}{P_P l\left(\|x\|\right)}\right\}\mathbb{1}_{I^x_{P\to P}<\eta}\right]$$

$$= \exp\left\{-\frac{\eta}{P_P l\left(\|x\|\right)}\right\} E\left[\exp\left\{\frac{I^x_{P\to P}}{P_P l\left(\|x\|\right)}\right\}\mathbb{1}_{I^x_{P\to P}<\eta}\right]. \tag{40}$$

The bound turns out as follows:

$$E\left[\exp\left\{\frac{I^x_{P\to P}}{P_P l\left(\|x\|\right)}\right\}\mathbb{1}_{I^x_{P\to P}<\eta}\right]$$

$$= E\Bigg[\prod_{i=1}^{+\infty}\Bigg(\exp\left\{\frac{\xi_i P_P l\left(\|Y_i\|\right)}{P_P l\left(\|x\|\right)}\right\}\mathbb{1}_{\|Y_i\|>\|x\|}$$

$$+ \mathbb{1}_{\|Y_i\|\leq\|x\|}\Bigg)\mathbb{1}_{I^x_{P\to P}<\eta}\Bigg] \tag{41}$$

$$\leq E\Bigg[\prod_{i=1}^{+\infty}\Bigg(\exp\left\{\frac{\xi_i l\left(\|Y_i\|\right)}{l\left(\|x\|\right)}\right\}\mathbb{1}_{\|Y_i\|>\|x\|}\mathbb{1}_{P_P\xi_i l(\|Y_i\|)<\eta}$$

$$+ \mathbb{1}_{\|Y_i\|\leq\|x\|}\Bigg)\Bigg]. \tag{42}$$

We use the probability generating function of the Poisson point process defined as:

$$E\left[\prod_{i=1}^{n} v_x(Y_i)\right] = \exp\left\{-\lambda_P \int_{\mathbb{R}^2} \left(1 - v_x(u)\right) du\right\} \tag{43}$$

with

$$v_x(u) = \exp\left\{\frac{\xi l\left(\|u\|\right)}{l\left(\|x\|\right)}\right\}\mathbb{1}_{\|u\|>\|x\|}\mathbb{1}_{P_P\xi l(\|u\|)<\eta} + \mathbb{1}_{\|u\|\leq\|x\|} \tag{44}$$

and we obtain:

$$E\left[\exp\left\{\frac{I^x_{P\to P}}{P_P l\left(\|x\|\right)}\right\}\mathbb{1}_{I^x_{P\to P}<\eta}\right] \leq \exp\Bigg\{-\lambda_P\int_{\mathbb{R}^2}\Bigg(1-E\Bigg[\Bigg(\exp\left\{\frac{\xi l\left(\|u\|\right)}{l\left(\|x\|\right)}\right\} \times \mathbb{1}_{\|u\|>\|x\|}\mathbb{1}_{P_P\xi l(\|u\|)<\eta}+\mathbb{1}_{\|u\|\leq\|x\|}\Bigg)\Bigg]\Bigg)du\Bigg\} \quad (45)$$

$$= \exp\Bigg\{-\lambda_P\int_{\mathbb{R}^2}\left(1-\mathbb{1}_{\|u\|\leq\|x\|}\right) - E\left[\exp\left\{\frac{\xi l\left(\|u\|\right)}{l\left(\|x\|\right)}\right\}\mathbb{1}_{P_P\xi l(\|u\|)<\eta}\right]\mathbb{1}_{\|u\|>\|x\|}du\Bigg\} \quad (46)$$

$$= \exp\Bigg\{-\lambda_P\int_{\|u\|>\|x\|}\Bigg(1-E\Bigg[\exp\left\{\frac{\xi l\left(\|u\|\right)}{l\left(\|x\|\right)}\right\} \times \mathbb{1}_{P_P\xi l(\|u\|)<\eta}\Bigg]\Bigg)du\Bigg\}. \quad (47)$$

We obtain,

$$E\left[\exp\left\{\frac{\xi l\left(\|u\|\right)}{l\left(\|x\|\right)}\right\}\mathbb{1}_{P_P\xi l(\|u\|)<\eta}\right]=\frac{1-\exp\left\{-\frac{\eta}{P_P}\left(\frac{1}{l(\|u\|)}-\frac{1}{l(\|x\|)}\right)\right\}}{1-\frac{l(\|u\|)}{l(\|x\|)}}. \quad (48)$$

Putting all of these together and changing for polar coordinates, we obtain:

$$P\left(I_{P\to P}\leq\eta\right)\geq 1-2\pi\lambda_P\int_0^{+\infty}\exp\Bigg\{-\frac{\eta}{P_P l(r)}-\lambda_P 2\pi \times\int_r^{+\infty}\Big(1-\frac{1-\exp\left\{-\frac{\eta}{P_P}\left(\frac{1}{l(w)}-\frac{1}{l(r)}\right)\right\}}{1-\frac{l(w)}{l(r)}}\Big)wdw\Bigg\}rdr. \quad (49)$$

The upper bound on the CCDF is then:

$$P\left(I_{P\to P}\geq\eta\right)\leq 2\pi\lambda_P\int_0^{+\infty}\exp\left\{-\frac{\eta}{P_P l(r)}\right\} \times\exp\Bigg\{-\lambda_P 2\pi\int_r^{+\infty}\Big(1-\frac{1-\exp\left\{-\frac{\eta}{P_P}\left(\frac{1}{l(w)}-\frac{1}{l(r)}\right)\right\}}{1-\frac{l(w)}{l(r)}}\Big)wdw\Bigg\}rdr. \quad (50)$$

Bound on $I_{P\to S}$. For $I_{P\to S}$, there is an inhibition ball $b(D,h_P)$ where we do not consider the points. Therefore, computations are similar to $I_{P\to P}$ except that we consider the points in $\mathbb{R}^2\backslash b(D,h_P)$. Formally, all the steps of the proof are the same, but we add an indicator function $\mathbb{1}_{Y_i\notin b(D,h_p)}$ equal to 1 if $Y_i\notin b(D,h_p)$ and 0 otherwise. It allows us to filter the points in $b(D,h_P)$.

Equation (36) can be written as:

$$P\left(I_{P\to S}\leq\eta\right) = 1-\sum_{k=1}^{+\infty}E\left[\exp\left\{-\frac{\eta-I^{k+1}_{P\to S}}{P_P l\left(\|Y_k\|\right)}\right\}\mathbb{1}_{I^{k+1}_{P\to S}<\eta}\mathbb{1}_{Y_k\notin b(D,h_P)}\right] \quad (51)$$

with

$$I^k_{P\to S}=\sum_{i=k}^{+\infty}P_P\xi_i l(\|Y_i\|)\mathbb{1}_{Y_i\notin b(D,h_P)}. \quad (52)$$

Equation (44) can be written as:

$$v_x(u)=\Bigg(\exp\left\{\frac{\xi l\left(\|u\|\right)}{l\left(\|x\|\right)}\right\}\mathbb{1}_{\|u\|>\|x\|}\mathbb{1}_{\|u-D\|>h_P}\mathbb{1}_{P_P\xi l(\|u\|)<\eta} +\left(1-\mathbb{1}_{\|u\|>\|x\|}\mathbb{1}_{\|u-D\|>h_P}\right)\Bigg) \quad (53)$$

and (47)

$$E\left[\exp\left\{\frac{I^x_{P\to S}}{P_P l\left(\|x\|\right)}\right\}\mathbb{1}_{I^x_{P\to S}<\eta}\right] \leq\exp\Bigg\{-\lambda_P\int_{\|u\|>\|x\|;\|u-D\|>h_P}\Bigg(1- E\left[\exp\left\{\frac{\xi l\left(\|u\|\right)}{l\left(\|x\|\right)}\right\}\mathbb{1}_{P_P\xi l(\|u\|)<\eta}\right]\Bigg)du\Bigg\}. \quad (54)$$

The upper bound on $I_{P\to S}$ CCDF is then:

$$P\left(I_{P\to S}\geq\eta\right)\leq\lambda_P\int_{\mathbb{R}^2\backslash b(D,h_P)}\exp\left\{-\frac{\eta}{P_P l(\|x\|)}\right\} \times\exp\Bigg\{-\lambda_P\int_{\|u\|>\|x\|;\|u-D\|>h_P}\Bigg(1- \frac{1-\exp\left\{-\frac{\eta}{P_P}\left(\frac{1}{l(\|u\|)}-\frac{1}{l(\|x\|)}\right)\right\}}{1-\frac{l(\|u\|)}{l(\|x\|)}}\Bigg)du\Bigg\}xdx. \quad (55)$$

Proof: Proof of Proposition 2

First, we compute the FER for a node at the origin and receiving a frame from a primary node at distance d as described in subsection II-C. We consider the FER for a transmission from a primary node. Computations for the secondary network is equivalent. We use the definition and method developed in [20]:

$$FER \;=\; P\left(SINR<\theta\right). \quad (56)$$

The $SINR$ is the ratio of the power received from the transmitter and the sum of the interference generated by the primary and secondary nodes plus noise. For a transmission from a Primary node, we get:

$$FER=P\left(\frac{\xi P_P l(d)}{I_{S\to P}+I_{P\to P}+W}<\theta\right) \quad (57)$$

$$=P\left(\xi<\frac{\theta}{P_P l(d)}(I_{S\to P}+I_{P\to P}+W)\right) \quad (58)$$

$$=1-E\left[\exp\left\{-\frac{\theta}{P_P l(d)}(I_{S\to P}+I_{P\to P}+W)\right\}\right]. \quad (59)$$

As we assumed that $I_{S\to P}$ and $I_{P\to P}$ were independent we get

$$FER=1-E\left[\exp\left\{-\frac{\theta}{P_P l(d)}I_{S\to P}\right\}\right] E\left[\exp\left\{-\frac{\theta}{P_P l(d)}I_{P\to P}\right\}\right]E\left[\exp\left\{-\frac{\theta}{P_P l(d)}W\right\}\right]. \quad (60)$$

The two Laplace transforms for $I_{S\to P}$ and W are obtained from

their distributions (log-normal for $I_{S\to P}$). For $I_{P\to P}$, we get:

$$E\left[\exp\left\{-\frac{\theta}{P_P l(d)} I_{P\to P}\right\}\right] = E\left[\exp\left\{-\frac{\theta}{P_P l(d)} \sum_{i=1}^{\infty} P_P \xi_i l\left(\|Y_i\|\right)\right\}\right] \quad (61)$$

$$= E\left[\prod_{i=1}^{n} \exp\left\{-\frac{\theta}{P_P l(d)} P_P \xi_i l\left(\|Y_i\|\right)\right\}\right]. \quad (62)$$

We use the probability generating function of the Poisson point process, we get:

$$E\left[\exp\left\{-\frac{\theta}{P_P l(d)} I_{P\to P}\right\}\right] = \exp\left\{-\lambda_P \int_{I\!R^2} \left(1 - E\left[\exp\left\{\frac{-\theta}{P_P l(d)} P_P \xi l\left(\|y\|\right)\right\}\right]\right) dy\right\} \quad (63)$$

$$= \exp\left\{-\lambda_P 2\pi \int_0^{+\infty} \left(1 - E\left[\exp\left\{\frac{-\theta}{P_P l(d)} P_P \xi l(r)\right\}\right]\right) r dr\right\} \quad (64)$$

$$= \exp\left\{-\lambda_P 2\pi \int_0^{+\infty} \frac{\theta l(r)}{l(d) + \theta l(r)} r dr\right\}. \quad (65)$$

REFERENCES

[1] Q. Zhao and B. Sadler, "A survey of dynamic spectrum access," *IEEE Signal Process. Mag.*, vol. 24, no. 3, pp. 79–89, 2007.

[2] B. Jabbari, R. Pickholtz, and M. Norton, "Dynamic spectrum access and management," *IEEE Wireless Commun. Mag.*, vol. 17, no. 4, pp. 6–15, 2010.

[3] J. Mitola, A. Attar, H. Zhang, O. Holland, H. Harada, and H. Aghvami, "Achievements and the road ahead: The first decade of cognitive radio," *IEEE Trans. Veh. Technol.*, vol. 59, no. 4, pp. 1574–1577, 2010.

[4] Y.-C. Liang, K.-C. Chen, Y. Li, P. Mahonen, and D. Niyato, "Advances in cognitive radio networking and communications," *IEEE J. Sel. Areas Commun.*, vol. 29, no. 2, pp. 273–493, 2011.

[5] I. F. Akyildiz, W. Y. Lee, M. C. Vuran, and S. Mohanty, "Next generation/dynamic spectrum access/cognitive radio wireless networks: A survey," *Comput. Netw.*, vol. 50, no. 13, pp. 2127–2159, 2006.

[6] Q. Zhao, L. Tong, A. Swami, and Y. Chen, "Decentralized cognitive mac for opportunistic spectrum access in ad hoc networks: A POMDP framework," *IEEE J. Sel. Areas Commun*, vol. 25, pp. 589–600, 2007.

[7] Y. Tevfik and H. Arslan, "A survey of spectrum sensing algorithms for cognitive radio applications," *IEEE commun. Surveys Tuts*, vol. 11, no. 1, pp. 116–130, 2009.

[8] F. Digham, M. Alouini, and M. Simon, "On the energy detection of unknown signals over fading channels," *IEEE Trans. Commun.*, vol. 55, no. 1, pp. 21–24, 2007.

[9] H. Sun, W.-Y. Chiu, A. Nallanathan, and H. V. Poor, "Wideband spectrum sensing with sub-nyquist sampling in cognitive radios," *IEEE Trans. Signal Process.*, vol. 60, no. 11, pp. 6068–6073, 2012.

[10] A. Babaei and B. Jabbari, "Throughput optimization in cognitive random wireless ad hoc networks," in *Proc. IEEE GLOBECOM*, 2010, pp. 1–5.

[11] Y. Liang, Y. Zeng, E. C. Peh, and A. T. Hoang, "Sensing-throughput tradeoff for cognitive radio networks," *IEEE Trans. Wireless Commun.*, vol. 7, no. 4, pp. 1326–1337, 2008.

[12] H. Li, Y. Gai, Z. He, K. Niu, and W. Wu, "Optimal power control game for cognitive radio networks with multiple interference temprature limits," in *Vehicular Technology Conference (VTC-Spring)*, 2008, pp. 1554–1558.

[13] A. Babaei and B. Jabbari, "Interference modeling and avoidance in spectrum underlay cognitive wireless networks," in *Proc. IEEE ICC*, 2010, pp. 1–5.

[14] S. Stotas and A. Nallanathan, "On the throughput and spectrum sensing enhancement of opportunistic spectrum access cognitive radio networks," *IEEE Trans. Wireless Commun.*, vol. 11, no. 1, pp. 97–107, 2012.

[15] Y. Wen, S. Loyka, and A. Yongacoglu, "On distribution of aggregate interference in cognitive radio networks," in *Proc. QBSC*, 2010, pp. 265–268.

[16] C.-H. Lee and M. Haenggi, "Interference and outage in poisson cognitive networks," *IEEE Trans. Wireless Commun.*, vol. 11, no. 4, pp. 1392–1401, 2012.

[17] A. Busson and G. Chelius, "Point processes for interference modeling in csma/ca ad-hoc networks," in *Proc. PE-WASUN*, 2009, pp. 33–40.

[18] D. Stoyan, W. Kendall, and J. Mecke, *Stochastic Geometry and Its Applications, 2nd Edition*. Chichester, UK: John Wiley and Sons Ltd, 1996.

[19] D. Daley and D. Vere-Jones, *An Introduction to the theory of point processes*. New York, USA: Springer-Verlag, 2003.

[20] F. Baccelli, B. Błaszczyszyn, and P. Mühlethaler, "An aloha protocol for multihop mobile wireless networks," *IEEE Trans. Inf. Theory*, vol. 52, no. 2, pp. 421–436, 2006.

[21] H. Nguyen, F. Baccelli, and D. Kofman, "A stochastic geometry analysis of dense ieee 802.11 networks," in *IEEE INFOCOM*, Anchorage, USA, 2007, pp. 1999–1207.

[22] R. Tandra, A. Sahai, and S. M. Mishra, "What is a spectrum hole and what does it take to recognize one?," *Proc. IEEE*, vol. 97, pp. 824–848, May 2009.

[23] A. Sahai, N. Hoven, and R. Tandra, "Some fundamental limits on cognitive radio," in *Forty-second Allerton Conference on Communication, Control, and Computing*, 2004.

[24] S. J. Shellhammer, N. Sai Shankar, R. Tandra, and J. Tomcik, "Performance of power detector sensors of DTV signals in IEEE 802.22 WRANS," in *Proc. TAPAS*, 2006.

[25] R. Tandra and A. Sahai, "SNR walls for signal detection," *IEEE J. Sel. Topics Signal Process.*, vol. 2, pp. 4–17, Feb. 2008.

[26] A. Busson, G. Chelius, and J.-M. Gorce, "Interference modeling in csma multi-hop wireless networks," Research Report RR-6624, INRIA, 2008.

[27] "IEEE 802.22 working group on wireless regional area networks enabling rural broadband wireless access using cognitive radio technology in tv whitespaces." [Online]. http://www.ieee802.org/22/.

[28] "Method for point-to-area communication for terrestrial services in the frequency range 30 mhz to 3000 mhz, itu-r p.1546-3," Jan. 2007.

[29] F. Baccelli and P. Brémaud, *Elements of Queueing Theory*. NY: Springer-Verlag, 2002.

Anthony Busson is a Full Professor at University Lyon 1 (Lyon-France). He is currently a member of the INRIA DANTE team in the Laboratoire de linformatique du Paralllisme. He received his Ph.D. degree in Computer Science from ENST (Ecole Nationale Suprieure des Tlcommunications, Paris) in 2002. He was Associate Professor at University Paris XI for 10 years, in the Institute of Fundamental Electronics and Laboratory of Signals and Systems. His research interests include performance evaluation, stochastic geometry, dynamic networks, mesh, and vehicular ad hoc networks.

Bijan Jabbari is a Professor in the Department of Electrical and Computer Engineering at George Mason University, Fairfax, Virginia, USA. He is also an Affiliated Faculty withTelecom Paris-Tech (ENST-Paris) in France. His area of specialization and interest is in wireless communication networks with particular emphasis on multi-user access, resource allocation, performance optimization, and cognitive radio networks. He is a Fellow of IEEE and received the IEE (UK) Fellow grade, the IEEE Millennium Medal and is a recipient of the Washington D.C. Metropolitan Area Engineer of the Year Award. He was recently selected as the recipient of the Outstanding Faculty Research Award from the School of Engineering of George Mason University. He served as the Editor for Wireless Multiple Access for the IEEE Transactions on Communications, was an International Division Editor for Wireless Communications of the Journal of Communications and Networks, and was on the editorial board of the Proceedings of the IEEE, as well as serving in different editorship capacity for several other journals. He is the past chairman of the IEEE Communications Society technical committee on Communications Switching and Routing. He has published extensively in the refereed journals and conferences. He spent his sabbatical leave at Seoul

National University in Korea in Spring 2011. He has founded innovative laboratories for Internet and wireless communications research. He has been an advisor to the industry, Government and European Commission. He received his M.S. and Ph.D. degrees in Electrical Engineering from Stanford University, Stanford, California.

Alireza Babaei received his B.S. and M.S. degrees in Electrical Engineering from K. N. Toosi University of Technology and Iran University of Science and Technology, Tehran, Iran in 2003 and 2005, respectively, and his Ph.D. degree in Electrical and Computer Engineering from George Mason University (GMU), Fairfax, Virginia, USA in 2009. He is currently a wireless architect at CableLabs. Prior to his current position, he was a Research Scientist in Wireless @ VT at Virginia Tech and a Postdoctoral Fellow in Auburn University. He is the recipient of an outstanding graduate student award from GMU, 2012 Journal of Communications and Networks best paper award, and the co-recipient of IEEE ICC 2012 wireless networking symposium best paper award. He has extensive publications in the areas of radio spectrum sharing, cognitive radio networks, and modeling and analysis of random wireless networks.

Véronique Vèque passed her M.S. degree in Computer Science from University Pierre et Marie Curie - France, in 09/1985. Under the supervision of Professor Guy Pujolle, she obtained her Ph.D. degree in Communication Networks in Dec. 1989 and its HDR in 1999. From Sept. 1989 to Aug. 2000, she was an Associate Professor at University of Paris Sud (Paris 11), France and a research member of Laboratory for Computer Science in Orsay. From Sept. 2000 to present, she worked as a Full Professor at University of Paris Sud. Since 2010, she joined the Laboratory of Signal and Systems in Supelec. Her research interests lie in the field of both wireless, mobile and high speed communication networks with emphasis on resource allocation, quality of service techniques, ad hoc routing and performance evaluation. She has supervised 13 Ph.D. theses. She is co-author of a book on high-speed networks and ATM techniques in 1995. She has published more than 65 papers in international journals or conferences. She is a Senior member of the IEEE, IEEE Communications Society, and IEEE Vehicular Society.